ICAS 2020 SHANGHAI
International Council of the Aeronautical Sciences
32nd Congress of the International Council of the Aeronautical Sciences
September 6-10, 2021
Pudong Shangri-La, Shanghai, China

INFLUENCE OF VARIABLE WALL PERFORATION RATIO ON BOUNDARY LAYER PARAMETERS AT TRANSONIC SPEEDS

Osipova S.L.[1,2]

[1]Central Aerohydrodynamic Institute (TsAGI), 1, Zhukovsky st., Moscow region, Zhukovsky 140180, Russia
[2]Institute of Physics and Technology (MIPT), 9, Institutsky lane, Moscow region, Dolgoprudny 141700, Russia

Abstract

This paper continues the series of experimental studies conducted in interchangeable test sections of T-128 TsAGI transonic wind tunnel. The results of measuring boundary layer longitudinal velocity profiles on the nozzle (solid) wall, on the upper and side walls of test sections #1, 2 (perforated walls) and #3 (slotted walls) are presented. The shape factor and friction coefficient were also obtained. Investigations were carried out in the Mach number range M = 0.2÷1.4 and Reynolds number range $Re_\theta \approx (1.0 \div 2.3) \cdot 10^5$. Reynolds number was related to momentum thickness — θ.

Keywords: turbulent boundary layer, wind tunnel testing, transonic flow, very high Reynolds numbers

1. Introduction

Studies of turbulent boundary layers (TBL) on solid surfaces at high Reynolds numbers cause both practical and fundamental interest [1]:

• useful for large aircraft and ships designers;

• there is still no answer what would happen to the TBL at $Re \to \infty$?

Investigations of TBL on perforated walls are equally interesting. Perforated surfaces are often used in the jet engines intakes and as the walls of test sections of transonic wind tunnels. Considering TBL on the wind tunnel test section perforated wall, its parameters could help to:

• find out how test section perforated walls influence on aircraft models aerodynamic characteristics. TBL parameters could be used to set boundary conditions in this class of problems [2];

• estimate the test section drag, which is important to design new wind tunnels;

• optimize moving test section elements position in existing facilities to improve the quality of the flow and minimize the drag of test section [3].

In its entirety, investigations of boundary layers on nozzles and test sections walls help to provide high flow field uniformity due to the optimal configuration of movable test section elements determining [4] and facility power consumption decreases [3]. This paper continues the series of experimental studies of turbulent boundary layers conducted in interchangeable test sections of T-128 TsAGI transonic wind tunnel.

In this report the turbulent boundary layer parameters (Clauser equilibrium parameter, skin friction coefficient, shape factor) were achieved by measuring longitudinal velocity profiles in TBL on the nozzle (solid) wall, on the upper and side walls of test sections #1, 2 (perforated walls) and #3 (slotted walls) are presented. Due to the lack of experimental data obtained on the permeable surfaces the aim of this work was to provide novel data on slotted and perforated surfaces at very high Reynolds numbers related to momentum thickness (up to $2.3 \cdot 10^5$) and to supplement the existing database on

the smooth surfaces.

2. Experimental set-up

The experiments were conducted in T-128 TsAGI facility. It is a closed-circuit wind tunnel with a four staged compressor of a 100 MW power (Fig.1).

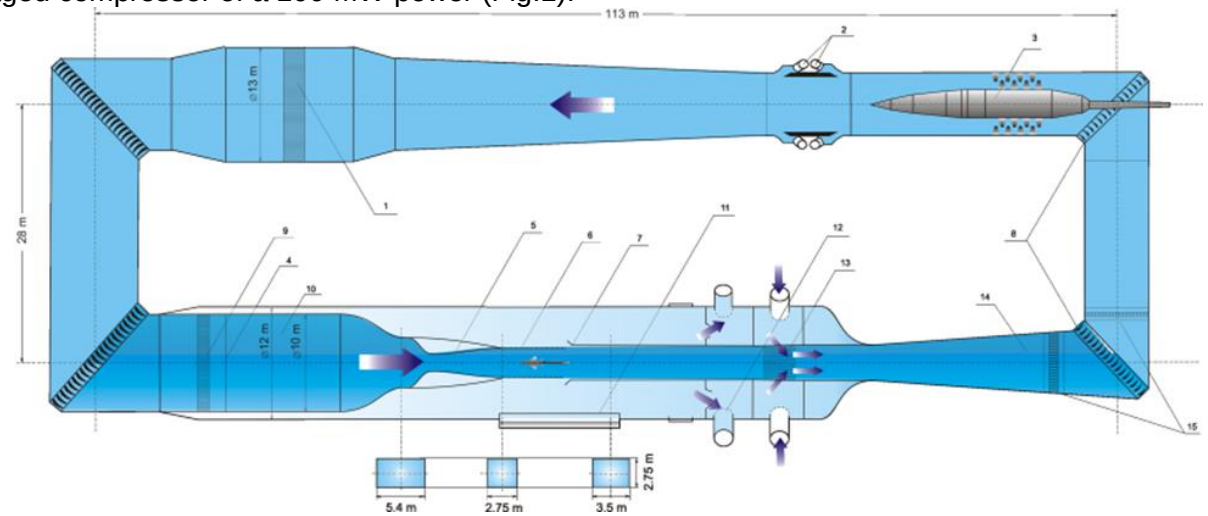

Figure 1 – T-128 wind tunnel scheme. 1 – cooler. 2 – flooding and vacuum-pumping system valves. 3 – compressor. 4 – deturbulising screens. 5 – variable nozzle. 6 – test section. 7 – mixing chamber flaps. 8 – turning blades. 9 – honeycomb. 10 – settling chamber. 11 – hatch for test section change. 12 – suction inlet in plenum chamber. 13 – suction outlet. 14 – diffuser. 15 – protecting screens.

T-128 circuit includes 4 interchangeable test sections with unique walls of adaptive permeability. The facility was described more thoroughly in [5]. In this investigation test sections #1, 2 with perforated walls and #3 — with slotted walls were used. Rakes of total pressure probes were mounted:

- on the nozzle upper wall (Fig.2): 23 probes, 0.17 m long;
- on the side wall of test section #1: 26 probes, 0.2 m long;
- on the upper wall of test section #2 (Fig.3) 22 probes, 0.29 m long;
- twice on the side wall of test section #3 (Fig.4): 22 probes, 0.13 m long and 24 probes, 0.29 m long.

Figure 2 – Rake mounted on the nozzle upper wall.

Figure 3 – Rake mounted on the upper wall of test section #2. Similar rake was mounted on the side wall of test section #1.

Figure 4 – Two rakes mounted on the side wall of test section #3.

During testing the parameters were varied as follows:

- Mach number in the range $M = 0.2 \div 0.8$;
- Reynolds number in the range $Re_\theta \approx (1.0 \div 2.3) \cdot 10^5$. It was changed by setting the total pressure values. Momentum thickness θ of the boundary layer was chosen as the characteristic scale;
- test sections #1, 2 walls perforation ratio ($f = 0 \div 10\%$) (Fig.5) and test section #3 slotted walls openness ratio ($f = 0 \div 3\%$);
- test sections #1, 2 panels divergence angle ($\alpha_{panel} = 0.5 \div 1°$) (Fig.6).

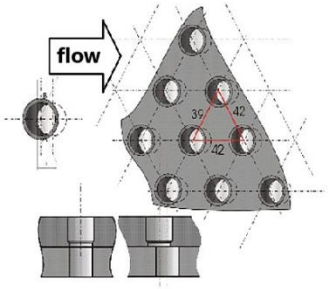

Figure 5 – Scheme of variable perforation on test sections #1 and #2.

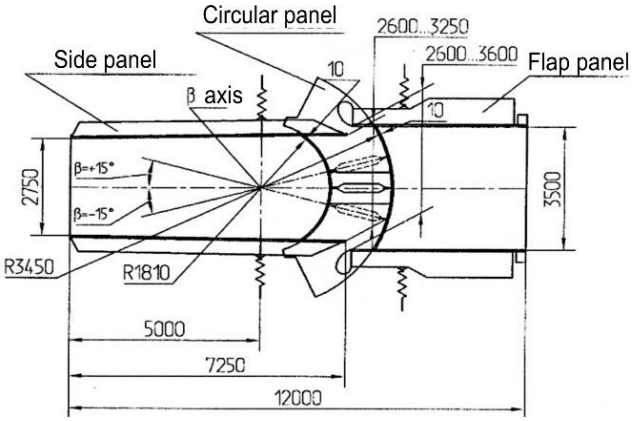

Figure 6 – Scheme of test section (TS) #1. Test section #2 has the same construction, except for the pitch sector: TS #2 is equipped with a strip suspension.

Were measured:

- main flow parameters (P_0, P_{st}, T_0);
- total pressure profiles in the boundary layer on the walls of nozzle and test sections #1, 2 and 3 (via total pressure probes);
- static pressure in the section where the rakes were located.

3. Results and discussion

3.1 Influence of Mach number on boundary layer parameters

TBL parameters obtained on the solid nozzle wall are in the Mach number range M = 0.2÷1.4. TBL parameters on the perforated walls of test section #1 and #2 were obtained at M = 0.7 and M = 0.8 respectively. TBL parameters on the slotted walls of test section #3 were obtained at M = 0.7 and M = 0.8. To investigate the compressibility effects when comparing our data with other researchers' results we related each parameter to its incompressible value, achieved at M = 0.2 at flow regime with the same perforation ratio f. We compared our data with the experimental results by Coles [6], Ozerov [7], Winter & Gaudet [8], Kornilov [9], Gordeyev [10], Hakkinen [11]; numerical results mentioned in the Wenzel et al. review [12]: by Alizard, Pirozoli, Li&Xi-Yun, Duan et al., Maeder et al., Mayer et al. and Wenzel et al. and some semi-empirical dependencies.

Firstly, to verify whether the boundary layer was equilibrium, we evaluated the Clauser equilibrium parameter G (Fig.7).

Data obtained in the T-128 nozzle, lie close to the experimental data by Ozerov and Winter & Gaudet in the range of Mach number M = 0.4÷0.8 and at M = 1.4 and matches the curve by Prandtl-Karman

(when c_f = 0.007) [13] in the range of Mach number M = 0.7÷1.0.

Data obtained on permeable walls of T-128 test sections #2 (perforated) and #3 (slotted) lie between the curves by Prandtl-Karman with c_f = 0.004 and c_f = 0.003. However, the value of G/G_0 for test section #1 lies approximately 20% higher than the other data obtained in T-128 and needs further thorough investigations.

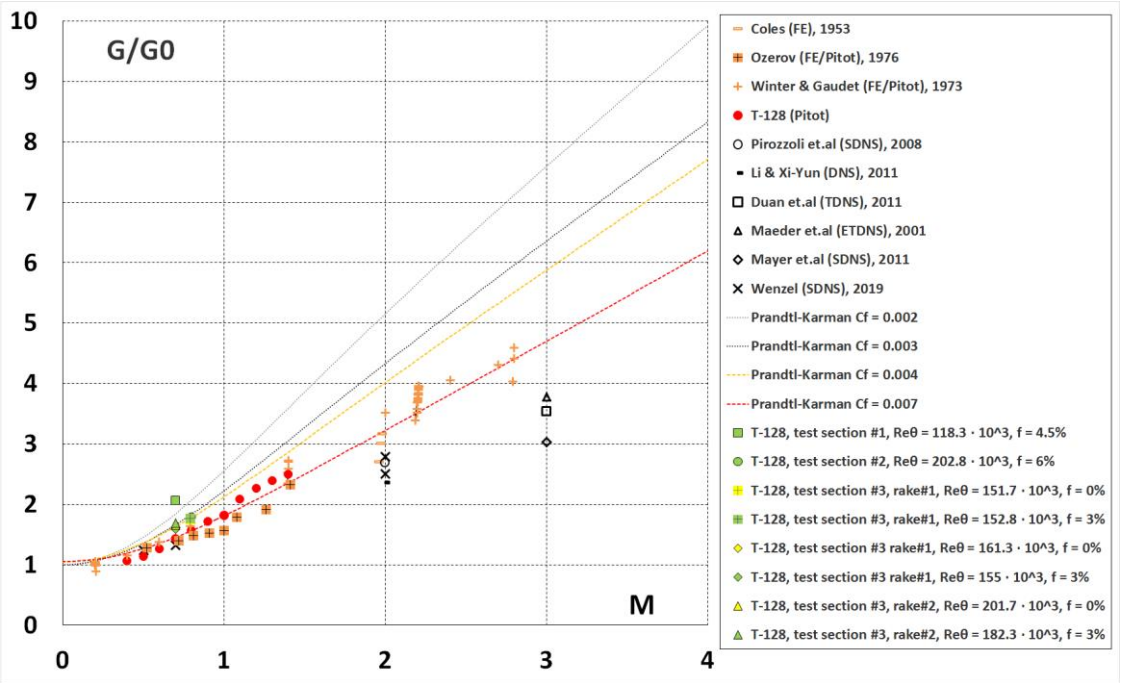

Figure 7 – *G/G0* as a function of *M*

Skin friction coefficient C_f was calculated by Clauser chart method. Constants in the classical logarithmic velocity profile were used as recommended by [14]: k = 0.384 and B = 4.17. The same k and B were used for smooth, perforated and slotted walls.

Fig. 8 shows the c_f/c_{f0} value obtained on the smooth nozzle wall of T-128 wind tunnel in comparison with the other researchers data. According to the semi-empirical dependencies of Reshotko $\frac{c_f}{c_{f0}} = (1 + 0.144M^2)^{-0.578}$ [15], Stratford & Beathers $\frac{c_f}{c_{f0}} = (1 + 0.16M^2)^{-0.6}$ [16], Prandtl-Schlichting $\frac{c_f}{c_{f0}} = 0.46 \cdot (\lg(Re_L \cdot \frac{T_w}{T}))^{-2.6}$ [17], Karman $\frac{c_f}{c_{f0}} = \frac{1-0.2 \cdot M^2}{0.2 \cdot M^2 \cdot (\arcsin(0.2^{M/2}))^2}$ [13], Loitsyanskiy (case (A) – $\frac{c_f}{c_{f0}} = (\frac{2}{2+\frac{\gamma-1}{2}M^2})^{5/7}$ – when boundary layer temperature is equal to mean value of flow and wall temperatures, $\mu \sim T^1$; case (B) – $\frac{c_f}{c_{f0}} = (\frac{1}{1+\frac{\gamma-1}{2}M^2})^{5/7}$ – when boundary layer temperature is set as the wall temperature; $\gamma = \frac{\kappa-1}{2}M^2\frac{T}{T_w}, \boldsymbol{\kappa = 1.4}$) [13], c_f/c_{f0} value tends to reduce with the growth of Mach number.

In the range of Mach number M = 0.4÷0.8 data obtained in T-128 lies between the curves by Loitsyanskiy (case (B)) and Reshotko; when $M \geq 0.9$ up to 1.4 – between the curves offered by Loitsyanskiy (case (A)) and Prandtl-Schlichting. At M = 1.1 and 1.2 data obtained in T-128 matches the Loitsyanskiy (case (A)) curve. However, further investigations are need to make other conclusions about the influence of Mach number on c_f/c_{f0} value.

Fig. 9 displays that shape factor ratio H/H_0 value smoothly increase with a growth of Mach number for

TBL on the all types of T-128 walls except for the test section #1: shape factor relation lies approximately 5.5% higher than the other obtained in T-128 data and needs further investigation.

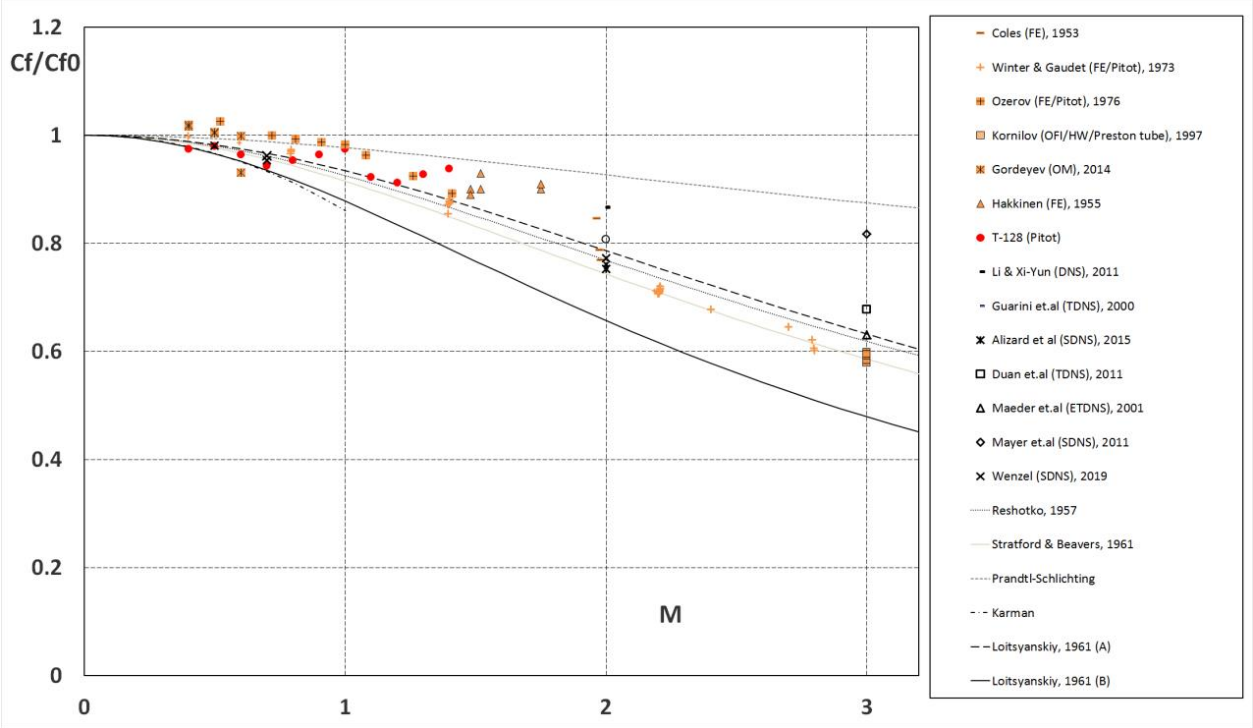

Figure 8 – c_f/c_{f0} as a function of M

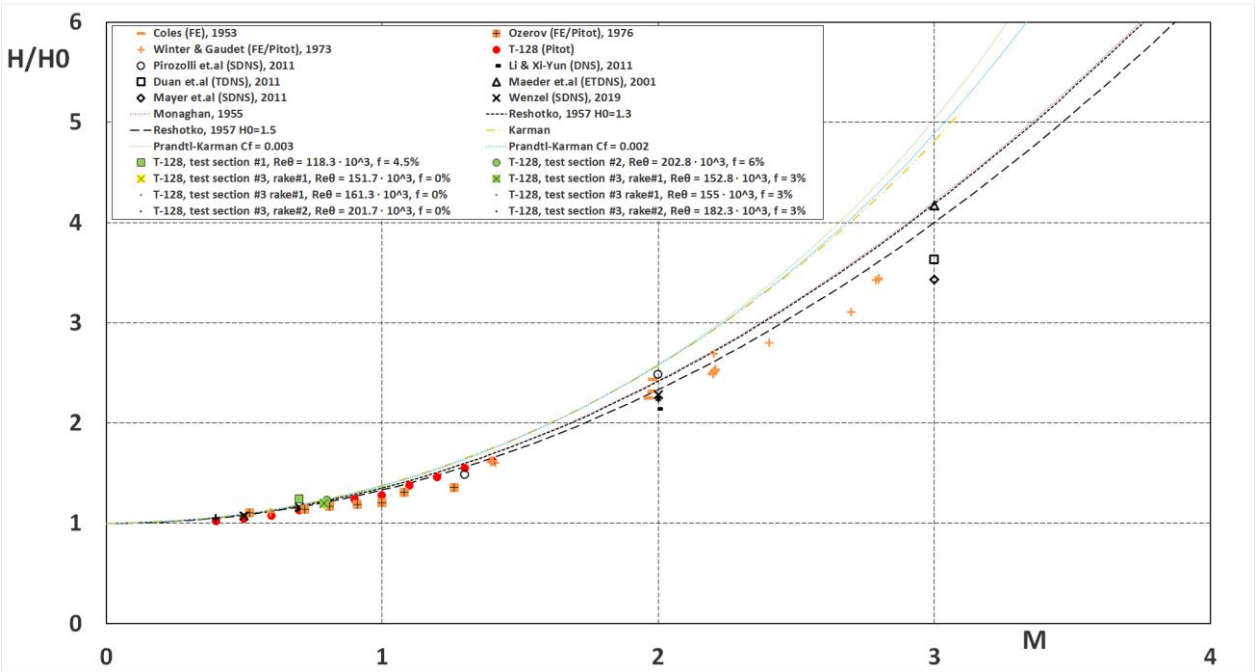

Figure 9 – H/H_0 as a function of M

H/H_0 obtained in T-128 wind tunnel agrees with other researchers numerically simulated, experimental data and semi-empirical dependencies by Karman [13], Monaghan $\frac{H}{H_0} = 1 + 0.89 \cdot (\gamma - 1) \cdot M^2$ [18] and Reshotko $\frac{H}{H_0} = 1 + \frac{\gamma-1}{2} M^2 \left(1 + {}^{1}/_{H_0}\right)$ [15]. The best match is with the curves by Reshotko

(especially when H_0 = 1.5).

3.2 Influence of perforation ratio on the boundary layer parameters

To investigate how perforation and openness ratios influence on the boundary layer parameters we grouped the data obtained on perforated and slotted walls of T-128 with close values of Reynolds number Re_θ: $Re_\theta = (120\pm15) \cdot 10^3$ and $Re_\theta = (210\pm15) \cdot 10^3$ for the perforated walls both of test sections #1 and #2, $Re_\theta = (170\pm15) \cdot 10^3$ for the slotted walls of test section #3.

Fig. 10 shows how the perforation ratio f influences on the Clauser equilibrium parameter G. For the perforated walls value of G tends to smoothly decrease with the growth of perforation ratio f in the range f = 0÷10%. The linear trends for both groups of data on the perforated wall at $Re_\theta = (120\pm15) \cdot 10^3$ and $Re_\theta = (210\pm15) \cdot 10^3$ has close tilt (-0.2432 and -0.227 respectively) and shift (16.023 and 17.854 respectively) coefficients. The $Re_\theta = (210\pm15) \cdot 10^3$ curve lies higher than the $Re_\theta = (120\pm15) \cdot 10^3$ curve.

As for the slotted walls, Clauser equilibrium parameter has no visible dependence on openness ratio f in the range f = 0÷3%. However, further investigations in the wider openness ratio are needed to spread these conclusions.

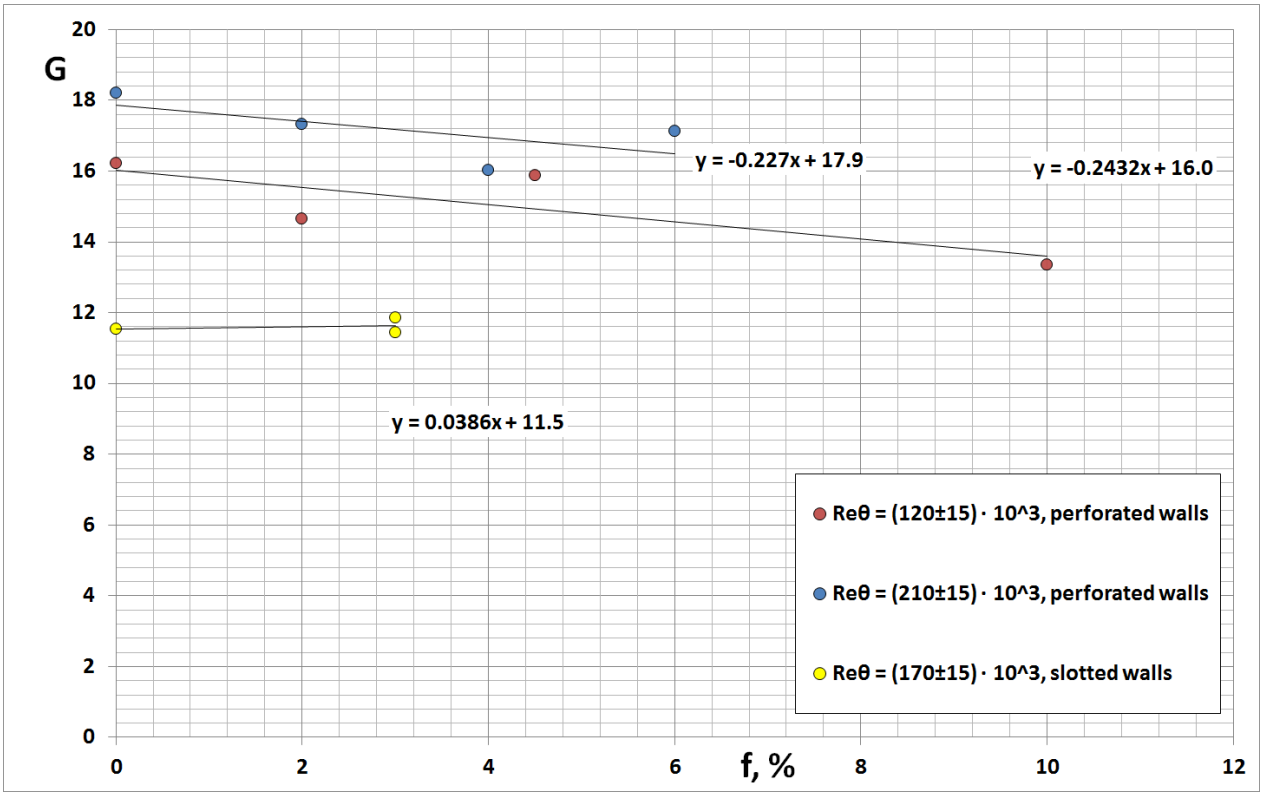

Figure 10 – Clauser equilibrium parameter G as a function of perforation ratio f

Fig.11 displays the influence of perforation ratio f on skin friction coefficient c_f. For the perforated walls value of C_f tends to smoothly increase with the growth of perforation ratio f in the range f = 0÷10%. The linear trends for both groups of data on the perforated wall at $Re_\theta = (120\pm15) \cdot 10^3$ and $Re_\theta = (210\pm15) \cdot 10^3$ has close tilt and shift (0,0011 and 0,001 respectively) coefficients. The $Re_\theta = (210\pm15) \cdot 10^3$ curve lies lower than the $Re_\theta = (120\pm15) \cdot 10^3$ curve.

At f = 0% skin friction coefficient c_f of TBL on the slotted walls is more than 40% bigger than c_f of TBL on the perforated walls. According to the obtained data it is hard to make any conclusion about c_f dependence on openness ratio f in the range f = 0÷3%. Further investigations are needed to discover any trends.

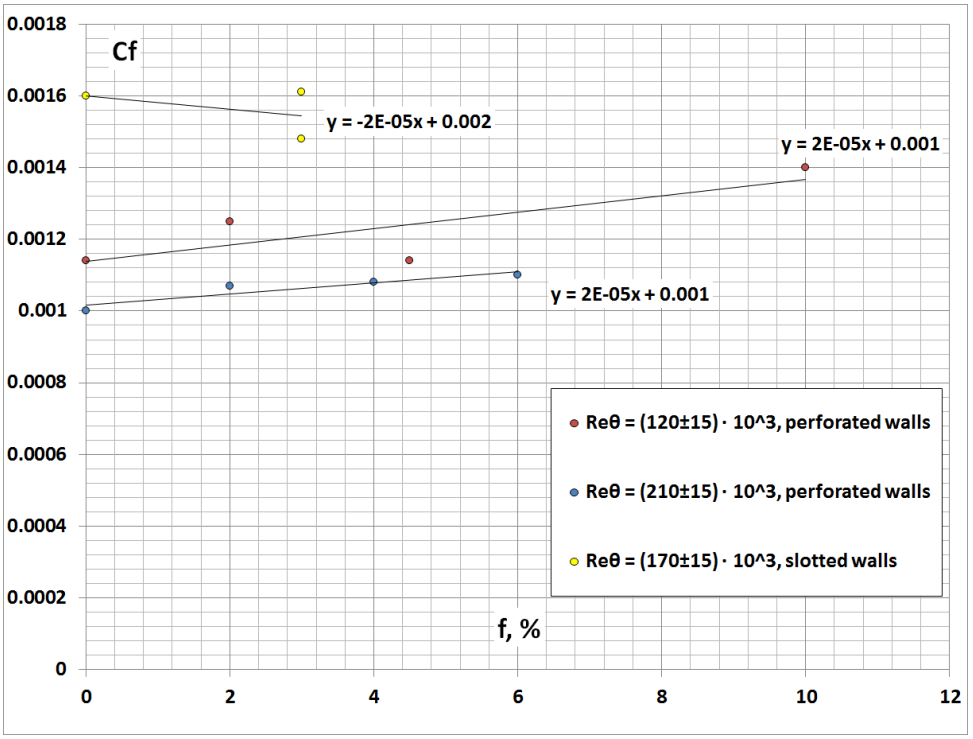

Figure 11 – Skin friction coefficient c_f as a function of perforation ratio f

Fig.12 shows the influence of perforation ratio f on shape factor H. For the perforated walls value of H has no significant dependence on perforation ratio f in the range f = 0÷10%. The linear trends for both groups of data on the perforated wall at Re_θ = (120±15) · 10^3 and Re_θ = (210±15) · 10^3 are similar. The Re_θ = (210±15) · 10^3 curve lies higher than the Re_θ = (120±15) · 10^3 curve. The difference between the values of H at the similar flow regimes with the same perforation ratio values does not exceed $\Delta H \approx 0{,}09$ (≈ 6%).

As for the slotted walls, shape factor H has no visible dependence on openness ratio f in the range f = 0÷3%. However, further investigations in the wider openness ratio are needed to spread these conclusions.

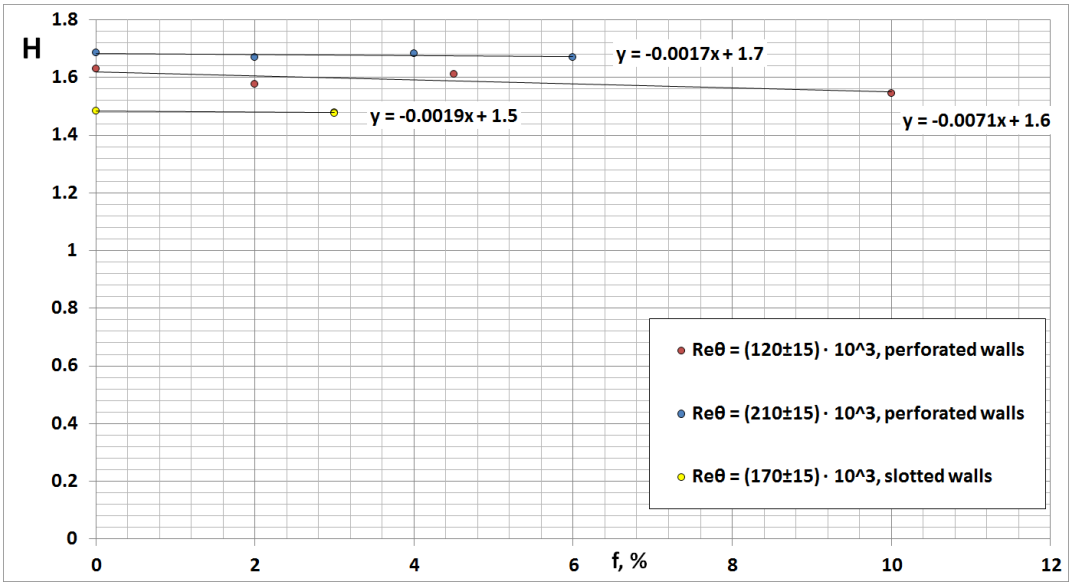

Figure 12 – Shape factor H as a function of perforation ratio f

4. Conclusions

The turbulent boundary layer parameters (Clauser equilibrium parameter, skin friction coefficient, shape factor) achieved by measuring longitudinal velocity profiles on the nozzle (solid) wall, on the upper and side walls of test sections #1, 2 (perforated walls) and #3 (slotted walls) are presented.

Novel data on slotted and perforated surfaces at very high Reynolds numbers related to momentum thickness (up to $2.3 \cdot 10^5$) are presented and the existing database on the smooth surfaces is supplemented.

The results of measurements of the boundary layer parameters on the smooth nozzle of T-128 wind tunnel were compared to the experimental data by Coles [6], Ozerov [7], Winter and Gaudet [8], Kornilov [9], Gordeyev [10], Hakkinen [11], numerically simulated results from the Wenzel et al. review [12] and semi-empirical dependencies by Reshotko [15], Stratford & Beathers [16], Prandtl-Schlichting [17], Karman [13], Loitsyanskiy [13], Monaghan [18], Prandtl-Karman [13]. Due to the lack of data on perforated and slotted surfaces it wasn't possible to compare data obtained in T-128 test sections #1, #2 and #3 with any experimental or numerical results.

First attempts to find out the trends of perforation ratio influence on the Clauser equilibrium parameter, skin friction coefficient and shape factor are made. However, further investigations in the wider perforation ratio are needed to verify and spread these conclusions.

Acknowledgements Experimental investigations were performed at the Central Aerohydrodynamic Institute. Author is grateful to S.A. Glazkov, A. R. Gorbushin, I.A. Sudakova and the whole team of T-128 wind tunnel.

Data processing was funded by RFBR, project number 19-38-90296. Analysis of data and preparation of manuscript were carried out with a grant from the Russian Science Foundation (project number 20-11-20006) at MIPT.

5. Contact Author Email Address

svetlana.l.osipova@tsagi.ru

6. Copyright Statement

References

[1] Gorbushin A., Osipova S. & Zametaev V. Mean Parameters of an Incompressible Turbulent Boundary Layer on the Wind Tunnel Wall at Very High Reynolds Numbers. *Flow, Turbulence and Combustion, 2020.* https://doi.org/10.1007/s10494-020-00232-z

[2] Glazkov S.A., Gorbushin A.R., Semenov A.V. et al. Influence of T-128 wind tunnel perforated walls on aerodynamic characteristics of reentry vehicles at transonic speed. CEAS Space J 12, 235–246, 2020. https://doi.org/10.1007/s12567-019-00293-5

[3] Glazkov S.A., Gorbushin A.R., Osipova S.L., Semenov A.V. Influence of movable test section elements configuration on its drag and flow field uniformity at transonic speeds // In-tern. *Conf. on the Methods of Aerophysical Research*, 2016. AIP Conference Proceedings 1770, 030008, 2016; http://dx.doi.org/10.1063/1.4963950.

[4] Biryukov V., Glazkov S., Gorbushin A., Ivanov A., Semenov A.: Experimental investigation of the effect of nozzle shape and test section perforation on the stationary and non-stationary characteristics of flow field in the large transonic TsAGI T-128 wind tunnel. *The Aeronautical Journal* (1968), 109(1092), 75-82

(2005). DOI:10.1017/S0001924000000579

[5] Burov V.V., Volobuev V.S., Glazkov S.A., Gorbushin A.R., Chumachenko E.K.: Measuring and computational system of TsAGI T-128 transonic wind tunnel. *Autom Remote Control* 72: 634, 2011. https://doi.org/10.1134/S0005117911030147

[6] Coles D.E. Measurements in a boundary layer on a smooth flat plate at a supersonic flow. Thesis in partial fulfillment of the requirements for the degree of Doctor of Philosophy. California Institute of Technology, Pasadena, California, 1953

[7] Ozerov V.N. Determination of skin friction coefficient using the results of measuring turbulent boundary layer velocity profiles at transonic speeds. *Uchenye zapiski TsAGI*, Vol.7, No.2, pp. 67–72, 1976

[8] Winter K.G., Gaudet L. Turbulent boundary-layer studies at high Reynolds numbers at Mach numbers between 0.2 and 2.8. ARC R&M 3712 London, pp. 1–57. Her Majesty's stationery office, 1973

[9] Kornilov V.I., Zharkova G.M., Lebiga V.A., Mironov S.G. Methods and instruments of flow investigations in aerogasodynamic experiment (review). *Thermophysics and Aeromechanics*, V.4, №3, pp. 283–294, 1997

[10] Gordeyev S., Smith A., Cress J., & Jumper E. Experimental studies of aero-optical properties of subsonic turbulent boundary layers. *Journal of Fluid Mechanics*, 740, pp. 214-253, 2014. DOI:10.1017/jfm.2013.658

[11] Hakkinen J. Raimo. Measurements of turbulent skin friction on a flat plate at transonic speeds. NACA TN 3486. California Institute of Technology. Washington, 1955.

[12] Wenzel C., Kloker M.J., Rist U. DNS of compressible turbulent boundary layers and assessment of data/scaling-law quality. *Journal of Fluid Mechanics*, 2018. DOI: 10.1017/jfm.2018.179

[13] Loitsyanskiy L.G. Mechanics of Liquids and Gases. Moscow, Nauka, 1987.

[14] H. Nagib, K. Chauhan, P. Monkewitz, Approach to an asymptotic state for zero pressure gradient turbulent boundary layers. Phil. Trans. R. Soc. A 365, 2007 https://doi:10.1098/rsta.2006.1948

[15]Reshotko E., Tucker M. Approximate calculation of the compressible boundary layer with heat transfer and arbitrary pressure gradient. NACA TN 4154, pp. 1–34. Lewis Flight Propulsion Laboratory, Cleveland, Ohio. Washington, 1957

[16]Stratford B.S & Beathers G.S. The Calculation of the Compressible Turbulent Boundary Layer in an Arbitrary Pressure Gradient-A Correlation of certain previous Methods. R. & M. No. 3207, London. Her Majesty's stationery office, 1961

[17]Schlichting H.: Boundary layer theory, vol. 7. McGraw-Hill, New York (1979)

[18]R.J. Monaghan M.A. A Review and Assessment of Various Formulae for Turbulent Skin Friction in Compressible Flow. C.P. No 142, TN No. Aero.2182, London. Her Majesty's stationery office, 1953